Weakly nonlinear analysis of long-wave Marangoni convection in a liquid layer covered by insoluble surfactant

Alexander B. Mikishev [*]
Dept. Engineering Technology, Sam Houston State University, Huntsville, Texas 77341, USA

Alexander A. Nepomnyashchy [†]
Department of Mathematics, Technion-Israel Institute of Technology, Haifa 32000, Israel

(Received 25 April 2019; published 19 September 2019)

We consider the long-wave Marangoni instability in a heated liquid layer covered by insoluble surfactant. The system of nonlinear equations derived in our previous work is regularized in the limit of strong surface tension. Recent research shows that, without the surfactant, a large-scale oscillatory instability mode exists in the interval of wave numbers $k = O(\mathrm{Bi}^{1/2})$ (the Biot number $\mathrm{Bi} \ll 1$). Here we study the influence of the surfactant on the Marangoni oscillations. The bifurcation analysis for traveling waves and counterpropagating waves is performed. The types of bifurcation and selected pattern depend on the elasticity number and on the Biot number. Specifically, at small elasticity number, both types of waves are supercritical.

DOI: 10.1103/PhysRevFluids.4.094002

I. INTRODUCTION

The formation and evolution of convective patterns generated by the Marangoni instability have been in the focus of numerous studies over recent years [1,2]. The case of long-wave instability, which is the subject of two extensive review papers [3,4], is of special interest. There are two basic factors that make the linear instability long-wave. The pioneering work of Pearson [5] shows that a liquid layer with poorly-heat-conducting boundaries is subject to a long-wave instability when heated from below. Another kind of long-wave Marangoni instability develops in very thin films or under microgravity conditions due to the free-surface deformation [6]. In both cases, the instability is monotonic and leads to the growth of large-scale disturbances on the liquid surface. The paper of Scanlon and Segel [7] was one of the first works where the nonlinear evolution of Marangoni patterns in a model liquid-gas system with semi-infinite phases and undeformable surface was investigated. The weakly nonlinear amplitude equation governing the long-wave deformational mode was derived in Refs. [8,9], while the strongly nonlinear amplitude equation was obtained by Davis [10]. For the deformational mode, a subcritical instability is typical, which leads to the rupture of the film. Most of the papers on the Marangoni convection in a layer with a poorly conducting upper boundary were carried out in the framework of the asymptotics $k \sim O(\mathrm{Bi}^{1/4})$, which has been found in Ref. [5]; here k is a wave number and Bi is the Biot number. For instance, that scaling was used in the paper of Golovin *et al.* [11], where the interfacial deformation effect on the nonlinear Marangoni pattern caused by the Pearson's long-wave instability was considered.

However, the Marangoni instability is not always monotonic. In the situation when the free surface of the liquid is covered by surface-active agent, under some conditions for the parameters the

[*] amik@shsu.edu
[†] nepom@technion.ac.il

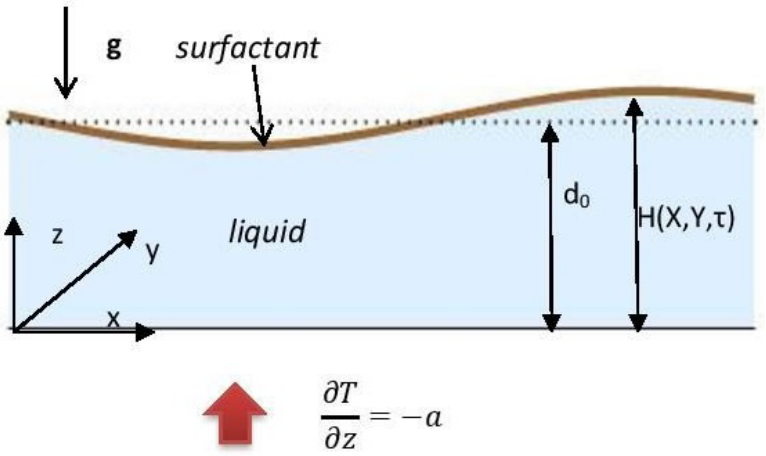

FIG. 1. A schematic of the physical problem considered in the paper. An insoluble surfactant is adsorbed at the deformable interface, $Z = H(X, Y, \tau)$. At the bottom of the liquid layer ($z = 0$) the temperature gradient $-a$ is applied.

most dangerous instability can be the oscillatory instability. The description of basic experiments on the Marangoni instability in the presence of surfactants can be found in review papers [4,12] and in Ref. [13]. The investigation of the long-wave Marangoni convection in the presence of a surfactant has been carried out in Ref. [14]. The authors performed the linear analysis of the Marangoni convection, found the instability thresholds of monotonic and oscillatory modes for nondeformable as well as for deformable liquid surfaces. Later, the nonlinear evolution equations for the scaling $k = O(\mathrm{Bi}^{1/4})$ were derived and bifurcation analysis near instability threshold was performed [15].

The recent work of Shklyaev *et al.* [16] shows the existence of the oscillatory instability mode when the liquid layer is heated from below and the critical perturbations are in the nonstandard range, $k \sim O(\mathrm{Bi}^{1/2})$, even without the surfactant. The influence of surfactant on the Marangoni oscillations is studied in the present work.

II. STATEMENT OF THE PROBLEM

We consider a liquid layer of the mean thickness d_0 heated from below (the temperature gradient a is applied) with a deformable free surface covered by a surfactant with a mean surface concentration Γ_0; see Fig. 1.

To obtain the equations for large-scale Marangoni convection in a liquid layer with insoluble surfactant on a deformable free surface we use the standard set of transport equations of mass, momentum, and energy with no-slip conditions for velocity and a specified heat flux condition on the bottom of the layer. At the free surface the boundary conditions are the kinematic boundary conditions, the Newton cooling law, the balance of both normal and tangential interfacial stresses and the distribution condition for the surfactant concentration.

The thermal diffusivity of the liquid is χ, the kinematic viscosity is ν, the density is ρ, the dynamic viscosity is $\eta = \nu\rho$, the surfactant diffusivity is D_0, the thermal conductivity of the liquid is Λ_T, the heat transfer coefficient at the free surface is q. It is assumed that the surface tension σ depends linearly on both temperature T and surfactant concentration Γ, $\sigma = \sigma_0 - \sigma_1(T - T_0) - \sigma_2(\Gamma - \Gamma_0)$ (σ_0 is the reference value of surface tension, $\sigma_1 = -\partial_T\sigma$, $\sigma_2 = -\partial_\Gamma\sigma$), which is reasonable if the disturbances of the temperature and concentration are sufficiently small. As the reference values of T and Γ, we choose their values at the surface in the absence of convection.

To rescale the variables of the problem we use the following units: length d_0, time d_0^2/χ, velocity χ/d_0, temperature ad_0, pressure $\rho\nu\chi/d_0^2$. The problem is characterized by the following

nondimensional parameters: $M = \sigma_1 a d_0^2/\eta\chi$ is the Marangoni number (thermocapillary surface forces via viscous forces), $N = \sigma_2 d_0 \Gamma_0/\eta\chi$ is the elasticity number (solutocapillary effects via viscous forces), $L = D_0/\chi$ is the Lewis number (mass diffusivity via thermal diffusivity), $G = g d_0^3/\nu\chi$ is the Galileo number (gravity forces via viscous forces), $S = \sigma_0 d_0/\chi\eta$ is the inverse capillary number (surface tension forces via viscous forces), $\mathrm{Bi} = q d_0/\Lambda_T$ is the Biot number (ratio of heat-transfer resistances inside of and at the surface of the liquid).

Later on, the Biot number is assumed to be small ($\mathrm{Bi} \ll 1$). The problem was considered in detail in the framework of linear stability theory under the assumption $k \sim \mathrm{Bi}^{1/4}$ [14]. Monotonic and oscillatory modes of long-wave instability were found. For a nondeformable upper free surface, the critical Marangoni number for the monotonic instability is

$$M_m = 48 + 12N/L,$$

and the oscillatory instability develops at

$$M_{\mathrm{osc}} = 48 + 12(4L + N),$$

with the frequency

$$\Omega_0 = (k^2/2)\sqrt{N - LN - 4L^2}.$$

In previous work [17], nonlinear amplitude equations governing the evolution of large-scale disturbances of surface deformation, temperature, and surfactant concentration were derived under the condition $S = O(1)$. All other nondimensional parameters, except Biot number, were also $O(1)$ and $\mathrm{Bi} = \beta\epsilon^4$. The obtained system was ill-posed, because it did not contain stabilizing terms with fourth-order spatial derivatives.

Marangoni oscillations can occur even without a surfactant. Shklyaev *et al.* [16] found the existence of a long-wave oscillatory instability mode in the interval of wave numbers $k \sim \mathrm{Bi}^{1/2}$. This result can be understood in the following way:

The "traditional" scaling $k \sim \mathrm{Bi}^{1/4}$ has been derived by Pearson [5] in the case of a *nondeformable interface* where, near the threshold, the instability is long-wave solely because of the small Biot number. This scaling can be obtained from the characteristic shape of the neutral curve,

$$M(k) = M_0 + a\mathrm{Bi}k^{-2} + ck^2, \tag{1}$$

which leads to the expression $k_c \sim (a\mathrm{Bi}/c)^{1/4}$ for the location of the neutral curve minimum. Here, a and c are some constants of the order of unity. For the Scriven-Sternling mode [6], which appears in the case of a *deformable interface*, the crucial factor which determines the characteristic spatial scale of the unstable disturbances, is the surface tension S which suppresses short-wave deformations. If $S \gg 1$, $c \sim S$ in expression (1), and the instability is long-wave even far from its threshold, i.e., for $M - M_0 = O(1)$. Assuming

$$\mathrm{Bi}k^{-2} \sim Sk^2 \sim 1$$

gives

$$k \sim \mathrm{Bi}^{1/2}, \quad S \sim k^{-2}.$$

The arguments presented above allow us to determine the appropriate scaling for the development of the nonlinear system of long-wave amplitude equations. First, let us rescale the horizontal coordinates x, y as

$$X = \epsilon x, \quad Y = \epsilon y, \quad 0 < \epsilon \ll 1,$$

which corresponds to disturbances with the wave number $k \sim \epsilon$. Because the characteristic frequency of waves $\omega \sim k^2$, the time variable is rescaled as $\tau = \epsilon^2 t$.

The appropriate scaling of the surface tension is $S = \epsilon^{-2}\tilde{\Sigma}$, $\tilde{\Sigma} = O(1)$, and that of the Biot number is $\mathrm{Bi} = \beta\epsilon^2$, i.e., $k \sim \mathrm{Bi}^{1/2}$ [16]. Later on, we refer to the oscillatory instability mode discovered in Ref. [16] as the *SAK mode*.

Applying the long-wave approach with the scaling described above, we obtain the following system of nondimensional amplitude equations for the local film thickness $H(X, Y, \tau)$, the surfactant concentration $\Gamma(X, Y, \tau)$, and perturbation of the free-surface temperature $F(X, Y, \tau)$:

$$\partial_\tau H = \nabla \cdot \left(\frac{H^3}{3}\nabla R + \frac{MH^2}{2}\nabla f + \frac{NH^2}{2}\nabla\Gamma \right) \equiv \nabla \cdot \mathbf{Q_1}, \tag{2}$$

$$H\partial_\tau F = \nabla \cdot \left(\frac{H^4}{8}\nabla R + \frac{MH^3}{6}\nabla f + \frac{NH^3}{6}\nabla\Gamma + H\nabla F \right) + \mathbf{Q_1} \cdot \nabla f - \frac{1}{2}(\nabla H)^2 - \beta f, \tag{3}$$

$$\partial_\tau \Gamma = \nabla \cdot \left[\Gamma H \left(\frac{H}{2}\nabla R + M\nabla f + N\nabla\Gamma \right) + L\nabla\Gamma \right] \equiv \nabla \cdot \mathbf{Q_2}. \tag{4}$$

Here,

$$R = GH - \tilde{\Sigma}\Delta H$$

is the pressure disturbance and

$$f = F - H$$

is the disturbance of the surface tension, $\nabla = (\partial_X, \partial_Y)$, $\Delta = \nabla \cdot \nabla$.

This problem is regularized by the strong surface tension, which suppresses shortwave disturbances. The set of equations (2)–(4) is a closed system which governs our problem. These equations describe the nonlinear dynamics of long-wave perturbations and include the following effects: On the right-hand side, Eq. (2) contains terms which describe the damping of the surface deformation due to gravity and surface tension and the influence of thermocapillary and solutocapillary effects on the layer thickness. The first two terms of Eq. (3) describe the advective heat transfer by the flow and heat conductivity in the longitudinal direction; the third and the fourth terms describe the heat loss from the free surface. Equation (4) describes the evolution of the surfactant concentration over the free surface of the liquid due to diffusion, surface deformation by gravity and surface tension, and by joint thermocapillary and solutocapillary effects.

III. LINEAR STABILITY THEORY

By definition, in the absence of convection $H = 1, \Gamma = 1$. According to Eq. (3), for any $\beta \neq 0$ the stationary value of F is equal to 1. Linearizing the system (2)–(4) around the base solution $H = F = \Gamma = 1$ with respect to long-wave disturbances $\sim \exp(\Lambda\tau + iKX) = \exp(\lambda t + ikx)$, where $k = \epsilon K$ is the wave number and $\lambda = \epsilon^2\Lambda$ is the growth rate, we obtain the cubic equation for $\Lambda(K) = \Lambda_r(K) + i\Lambda_i(K)$,

$$\begin{aligned}
0 &= \Lambda^3 + a_1\Lambda^2 + a_2\Lambda + a_3, \\
a_1 &= \tfrac{1}{3}K^2(3 + G + 3L - M + 3N + K^2S) + \beta, \\
a_2 &= \tfrac{1}{144}(K^4\{-24[2L(-3 + M) + 3(M - 2N)] + G(48 + 48L - M + 12N) \\
&\quad + K^2(48 + 48L - M + 12N)S\} + 48K^2[G + 3(L + N) + K^2S]\beta), \\
a_3 &= \tfrac{1}{144}(K^6\{-72LM + G[-L(-48 + M) + 12N] + K^2[-L(-48 + M) + 12N]S\} \\
&\quad + 12K^4(4L + N)(G + K^2S)\beta).
\end{aligned} \tag{5}$$

This equation can have both real and complex roots. For the monotonic instability mode we obtain the neutral stability curve [$\Lambda_r(K, M) = \Lambda_i(K, M) = 0$]

$$M_m(K) = \frac{(48 + 12N/L)(G + K^2\tilde{\Sigma})(\beta + K^2)}{K^2(72 + G + K^2\tilde{\Sigma})}. \tag{6}$$

In the case $\beta = 0$, it gives $M_m \to 48 + 12N/L$ as $G \to \infty$ (in the limit of a nondeformable surface) and $M_m \to \frac{12G(4L+N)}{L(72+G)}$ for $K \to 0$ for a deformable upper surface; see Ref. [14]. Also, the analysis reveals the existence of the oscillatory neutral stability curve [$\Lambda_r(K, M) = 0$, $\Lambda_i(K, M) \neq 0$]

$$M_{os} = \frac{\mathcal{D}_{11} - \sqrt{\mathcal{D}_{12}}}{2K^2(72 + G + 48L + K^2\tilde{\Sigma})}, \tag{7}$$

where

$$\begin{aligned}
\mathcal{D}_{11} &= 3(72 + 17G + 96L + 48N)\beta + K^2\{G^2 + 3G(41 + 32L + 5N) \\
&\quad + 72[3 + 5N + 2L(2 + L + N)] + 51\beta\tilde{\Sigma}\} + K^4(123 + 2G + 96L + 15N)\tilde{\Sigma} + K^6\tilde{\Sigma}^2, \\
\mathcal{D}_{12} &= \mathcal{D}_{11}^2 - 48(72 + G + 48L + K^2\tilde{\Sigma})[G + 3(L + N) + K^2\tilde{\Sigma}] \\
&\quad \times \{4K^2[G + 3(2 + L + N)]\beta + 12\beta^2 + K^6(4 + 4L + N)\tilde{\Sigma} \\
&\quad + K^4[12(1 + L + N) + G(4 + 4L + N) + 4\beta\tilde{\Sigma}]\}.
\end{aligned} \tag{8}$$

On the oscillatory instability boundary, the squared neutral frequency is

$$\begin{aligned}
\Omega_0^2 &= \tfrac{1}{288}(9K^2(5G + 16N - 24)\beta - K^4\{G^2 - 9G(N - 3) + 72[2L(N + L) + N + 3] \\
&\quad - 45\tilde{\Sigma}\beta\} + K^6(9N - 2G - 27)\tilde{\Sigma} - K^8\tilde{\Sigma}^2 + K^2\sqrt{\mathcal{D}_2}),
\end{aligned} \tag{9}$$

where

$$\begin{aligned}
\mathcal{D}_2 &= -144K^2(K^2\{-N(G + K^2\tilde{\Sigma})(72 + G + K^2\tilde{\Sigma}) + LN[864 + 36G + G^2 \\
&\quad + 2(18 + G)K^2\tilde{\Sigma} + K^4\tilde{\Sigma}^2] + 4L^2[216 + 27G + G^2 + (27 + 2G)K^2\tilde{\Sigma} + K^4\tilde{\Sigma}^2]\} \\
&\quad - \{36LN[-24 + G + K^2\tilde{\Sigma}] + N[G + K^2\tilde{\Sigma}][72 + G + K^2\tilde{\Sigma}] + 36L^2[-24 \\
&\quad + 5G + 5K^2\tilde{\Sigma}]\}\beta) + (K^4\{27 + 2G - 9N\}\tilde{\Sigma} + K^6\tilde{\Sigma}^2 - 9\{-24 + 5G + 16N\}\beta \\
&\quad + K^2\{G^2 - 9G[N - 3] + 72[3 + N + 2L(L + N)] - 45\tilde{\Sigma}\beta\})^2.
\end{aligned}$$

The detailed analysis of the problem in the absence of surfactant was performed by Shklyaev and coauthors in Ref. [16]. Here we show how the surfactant changes their results, especially for oscillatory mode. To be consistent with results of Shklyaev, we fix the inverse capillary number to unity, i.e., $\tilde{\Sigma} = 1$, without loss of generality (the choice corresponds to the definition $\epsilon \equiv S^{-1/2}$). It is known that typical values of the Lewis number of surfactants are small; later on, we take $L = 0.003$. Its influence on the oscillatory instability is not significant and the crucial parameter describing the influence of the surfactant on the stability is the elasticity parameter N.

The typical marginal stability curves in the case without the surfactant are presented in Fig. 2(a). Here solid lines correspond to the monotonic instability mode and dashed lines correspond to boundaries of oscillatory instability. It is seen that, without surfactant, the oscillatory mode appears for sufficiently large values of parameter β in a limited range of wave numbers. Shklyaev with coauthors [16] found that this mode is critical under the conditions

$$\beta\tilde{\Sigma} > 17.4, \quad G < 17.2. \tag{10}$$

Note that the interval of K with the oscillatory behavior of disturbances is wider than the oscillatory instability interval. In Fig. 2(b), the plots of $\Lambda_r(M)$ and $\Lambda_i(M)$ for $\beta = 40$ are shown for $K = 2$. One can see that, in a certain interval of M, $\Lambda_i \neq 0$ but $\Lambda_r < 0$, so there is no oscillatory

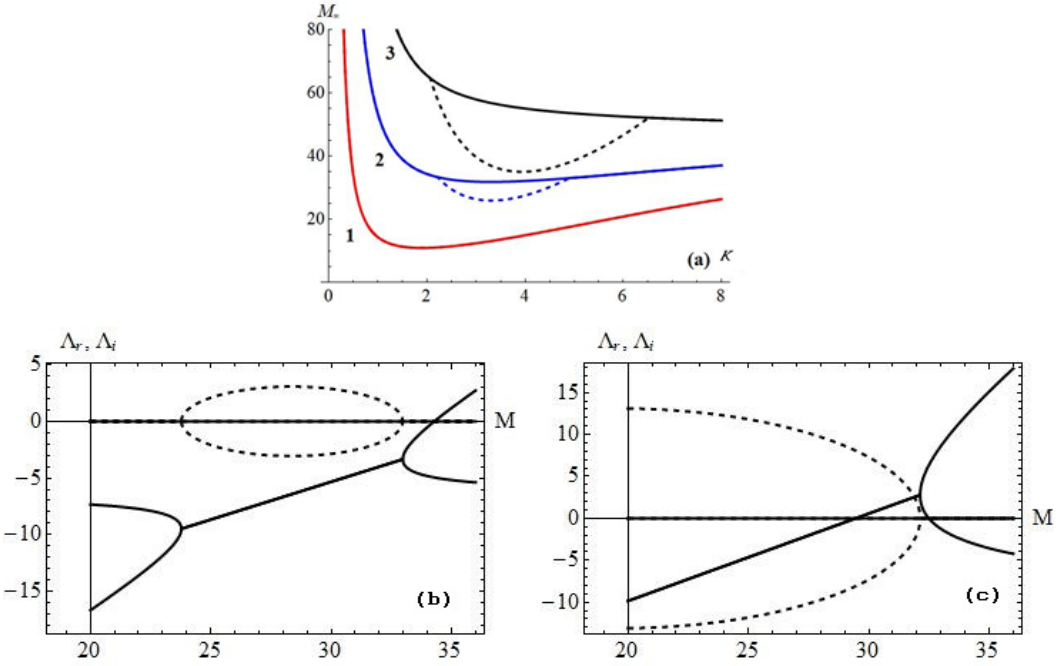

FIG. 2. (a) Marginal stability curves. The solid lines correspond to monotonic mode, the dashed lines correspond to oscillatory mode. Here $G = 1$ and $\beta = 10$, 40, and 80 for lines 1, 2, and 3, respectively. (b) Growth rate versus Marangoni number at fixed wave number $K = 2$. The solid lines correspond to the real part of the growth rate, Λ_r, the dashed lines correspond to the imaginary part, Λ_i. Here $G = 1$ and $\beta = 40$. (c) Growth rate versus Marangoni number at fixed wave number $K = 2.5$. The notation and values of parameters are the same as in panel (b).

instability. The dependencies $\Lambda_r(M)$ and $\Lambda_i(M)$ in the case of oscillatory instability ($\beta = 40$, $K = 2.5$) are shown in Fig. 2(c). Now Λ_r changes its sign in the interval of M where $\Lambda_i \neq 0$, which correspond to an oscillatory instability. The meaning of the monotonic marginal curve is changed with the growth of M, by crossing $M_m(K)$, one of unstable monotonic modes becomes stable.

However, even a rather small quantity of insoluble surfactant on the free surface creates a new type of oscillatory instability, which makes the oscillatory instability mode the most dangerous one for the full range of wave numbers, i.e., for all wave numbers the marginal curves for oscillatory mode are below the monotonic ones [see Fig. 3(a)]. In Fig. 3(b), the dependencies $\Lambda_r(M)$ and $\Lambda_i(M)$ are shown for $\beta = 40$, $K = 2$. Two different intervals where disturbances are oscillatory correspond to the decaying SAK mode and the surfactant-induced mode, which creates the oscillatory instability. Note that the latter mode exists in an interval of M which is much narrower than that of the existence of the former mode, and it is characterized by significantly smaller values of frequency Λ_i. For $K = 2.5$ [Fig. 3(c)], both intervals merge, and the threshold of the oscillatory instability is rather close to that obtained in the absence of the surfactant [see Fig. 2(c)]. Note however, that growth rates shown in Fig. 2(c) are two roots of a quadratic equation (no disturbances of Γ), while Fig. 3(c) shows three roots of the cubic equation (5). That leads to the appearance of an additional monotonic mode. The critical values of the monotonic Marangoni number are $M_m = 37.14$ at $K = 2$ and $M_m = 35.20$ at $K = 2.5$; the critical oscillatory Marangoni number is $M_{\text{osc}} = 34.31$ at $K = 2$ and $M_{\text{osc}} = 29.45$ at $K = 2.5$. The separation gap between monotonic and oscillatory instability curves increases when the elasticity parameter N grows.

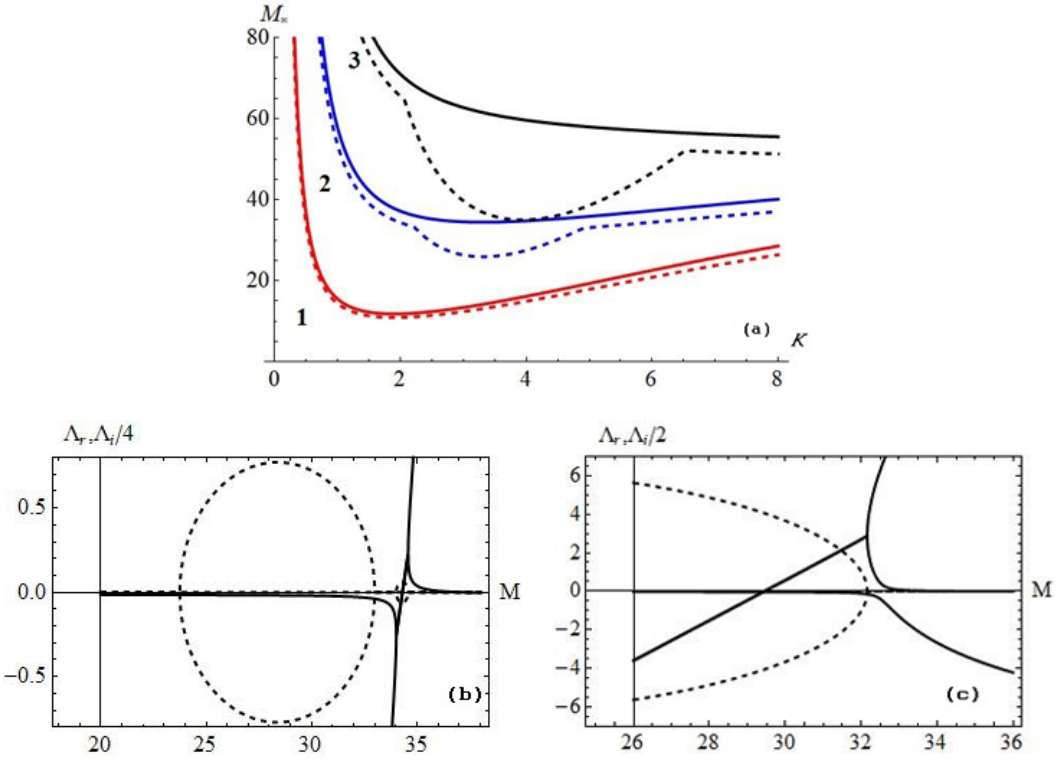

FIG. 3. (a) Marginal stability curves at $G = 1N = 0.001$, $L = 0.003$, and $\beta = 10$, 40, and 80 for lines 1, 2, and 3, respectively. The notations are the same as in Fig. 2(a). (b) Growth rate versus Marangoni number at fixed wave number $K = 2$ at $G = 1$, $S = 1$, $L = 0.003$, $N = 0.001$, and $\beta = 40$. The notations are the same as in Fig. 2(b). (c) Growth rate versus Marangoni number at fixed wave number $K = 2.5$. The notation and values of parameters are the same as in panel (b).

Let us minimize the marginal curves with respect to the rescaled wave number K for different values of the parameter β. The variations of the critical oscillatory Marangoni number as well as the critical wave number K are shown in Figs. 4(a) and 4(b), respectively. Here the elasticity parameter is fixed at $N = 0.001$. The jump of the critical wave number is explained in Fig. 5. When parameter β approaches 22.95, a new local minimum appears and, for β greater than 22.95, it becomes the global one. In Fig. 5 the solid line represents the minimum of the marginal curve at $\beta = 22.9$ (the global minimum is at $K_c = 2.58$), and the dashed line is for the marginal curve at $\beta = 23$ (the

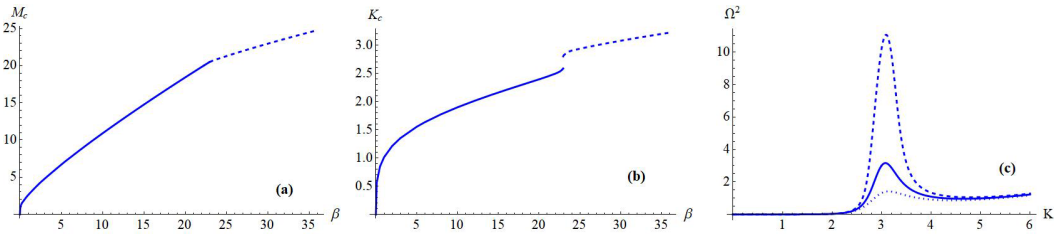

FIG. 4. (a) Variation of critical Marangoni number of the oscillatory mode. (b) Critical wave number K_c with parameter β. (c) Example of squared frequency jump, the solid line is for $\beta = 22$, the dashed line is for $\beta = 23$, and the dotted line is for $\beta = 21$. Other parameters are $G = 1$, $\tilde{\Sigma} = 1$, $L = 0.003$, and $N = 0.001$.

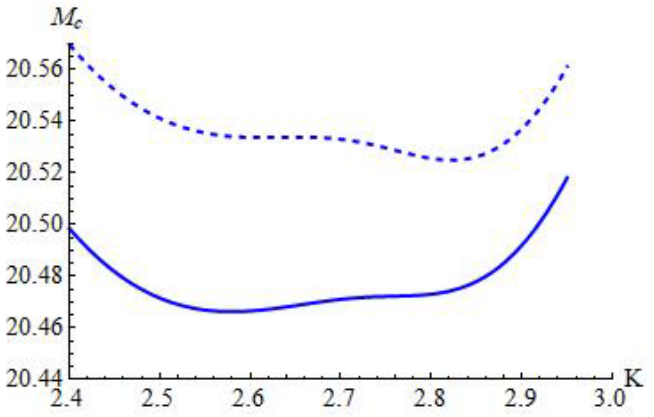

FIG. 5. Near the minimum of the critical Marangoni numbers at different β. The solid line is for $\beta = 22.9$, the dashed curve is for $\beta = 23$. Other parameters are $G = 1$, $\tilde{\Sigma} = 1$, $L = 0.003$, and $N = 0.001$.

global minimum is at $K_c = 2.82$). Together with the critical-wave-number jump we observe the jump of squared frequency of oscillatory perturbations. Figure 4(c) shows the squared frequency as a function of K for three different values for the parameter β: $\beta = 21$ (dotted line), $\beta = 22$ (solid line), and $\beta = 23$.

In the next section, we carry out the weakly nonlinear analysis of the problem. We consider the bifurcation of wave solution in the vicinity of the minimum of the oscillatory neutral curve.

IV. WEAKLY NONLINEAR ANALYSIS: TRAVELING WAVES

In the present paper we consider one-dimensional solutions, i.e., we assume that the solutions do not depend on Y.

We study the nonlinear dynamics in the vicinity of the oscillatory neutral curve, i.e., assuming small supercriticality of the Marangoni number,

$$M = M_0 + \delta^2 M_2,$$

where δ is a small parameter.

Here M_0 is the oscillatory instability threshold determined by Eq. (7). We introduce two temporal scales, $\tau_0 = \tau$ and $\tau_2 = \delta^2 \tau$, so that

$$\partial_\tau = \partial_{\tau_0} + \delta^2 \partial_{\tau_2}, \tag{11}$$

and expand the fields of film thickness, temperature, and surfactant concentration in powers of δ:

$$H = 1 + \delta h_1(X, \tau_0, \tau_2) + \cdots, \quad F = 1 + \delta\theta_1(X, \tau_0, \tau_2) + \cdots, \quad \Gamma = 1 + \delta\gamma_1(X, \tau_0, \tau_2) + \cdots. \tag{12}$$

Substituting this ansatz into Eqs. (2)–(4) and collecting terms of the same order of δ we obtain at first order the following linear problem:

$$h_{1,\tau_0} = \frac{1}{3}(Gh_1 - \tilde{\Sigma}h_{1,XX})_{XX} + \frac{M_0}{2}(\theta_1 - h_1)_{XX} + \frac{N}{2}\gamma_{1,XX}, \tag{13}$$

$$\theta_{1,\tau_0} = \frac{1}{8}(Gh_1 - \tilde{\Sigma}h_{1,XX})_{XX} + \frac{M_0}{6}(\theta_1 - h_1)_{XX} + \frac{N}{6}\gamma_{1,XX} + \theta_{1,XX} - \beta(\theta_1 - h_1), \tag{14}$$

$$\gamma_{1,\tau_0} = \tfrac{1}{2}(Gh_1 - \tilde{\Sigma}h_{1,XX})_{XX} + M_0(\theta_1 - h_1)_{XX} + (N + L)\gamma_{1,XX}, \tag{15}$$

where we use M_0 from Eq. (7).

The simplest solution of this system can be taken as a single traveling wave, i.e.

$$h_1 = H_1(\tau_2)e^{iKX+i\Omega_0\tau_0} + \text{c.c.}, \tag{16}$$

$$\theta_1 = \alpha_1 H_1(\tau_2)e^{iKX+i\Omega_0\tau_0} + \text{c.c.}, \tag{17}$$

$$\gamma_1 = \alpha_2 H_1(\tau_2)e^{iKX+i\Omega_0\tau_0} + \text{c.c.} \tag{18}$$

Here, "c.c." means complex-conjugate terms, and α_1 and α_2 can be obtained from the linear system (13)–(15) as

$$\alpha_1 = -\frac{GK^2 + \tilde{\Sigma}K^4 - 72\beta - 24i\Omega_0}{72(K^2 + \beta + i\Omega_0)}, \tag{19}$$

$$\alpha_2 = \frac{GK^2 + K^4\tilde{\Sigma} + 12i\Omega_0}{6K^2L + 6i\Omega_0}. \tag{20}$$

At second order, we obtain

$$\begin{aligned} &h_{2,\tau_0} - \frac{1}{3}(Gh_2 - \tilde{\Sigma}h_{2,XX})_{XX} - \frac{M_0}{2}(\theta_2 - h_2)_{XX} - \frac{N}{2}\gamma_{2,XX} \\ &\quad = G(h_1h_{1,X})_X - \tilde{\Sigma}(h_1h_{1,XXX})_X + M_0[h_1(\theta_1 - h_1)_X]_X + N(h_1\gamma_{1,X})_X, \end{aligned} \tag{21}$$

$$\begin{aligned} &\theta_{2,\tau_0} - \frac{1}{8}(Gh_2 - \tilde{\Sigma}h_{2,XX})_{XX} - \frac{M_0}{6}(\theta_2 - h_2)_{XX} - \frac{N}{6}\gamma_{2,XX} - \theta_{2,XX} + \beta(\theta_2 - h_2) \\ &\quad = \frac{3}{8}h_1(Gh_1 - \tilde{\Sigma}h_{1,XX})_{XX} + \frac{1}{3}\theta_{1,X}(Gh_1 - \tilde{\Sigma}h_{1,XX})_X + \frac{1}{6}h_{1,X}(Gh_1 - \tilde{\Sigma}h_{1,XX})_X \\ &\qquad + \frac{N}{3}h_1\gamma_{1,XX} + \frac{N}{2}\theta_{1,X}\gamma_{1,X} + \frac{M_0}{3}h_1(\theta_1 - h_1)_{XX} + \frac{M_0}{2}\theta_{1,X}(\theta_1 - h_1)_X \\ &\qquad + \theta_{1,X}h_{1,X} - \frac{1}{2}(h_{1,X})^2 + \beta h_1(\theta_1 - h_1), \end{aligned} \tag{22}$$

$$\begin{aligned} &\gamma_{2,\tau_0} - \frac{1}{2}(Gh_2 - \tilde{\Sigma}h_{2,XX})_{XX} - M_0(\theta_2 - h_2)_{XX} - (N + L)\gamma_{2,XX} \\ &\quad = (Gh_1h_{1,X} - \tilde{\Sigma}h_1h_{1,XXX})_X + \frac{1}{2}(G\gamma_1h_{1,X} - \tilde{\Sigma}\gamma_1h_{1,XXX})_X \\ &\qquad + M_0[(h_1 + \gamma_1)(\theta_1 - h_1)_X]_X + N[h_1 + \gamma_1)\gamma_{1,X}]_X. \end{aligned} \tag{23}$$

Here the solution has the form

$$h_2 = H_2(\tau_2)e^{2iKX+2i\Omega_0\tau_0} + \text{c.c.}, \tag{24}$$

$$\theta_2 = F_0 + F_2(\tau_2)e^{2iKX+2i\Omega_0\tau_0} + \text{c.c.}, \tag{25}$$

$$\gamma_2 = \Gamma_2(\tau_2)e^{2iKX+2i\Omega_0\tau_0} + \text{c.c.} \tag{26}$$

The solvability condition at the third order of the expansion in powers of δ determines the Landau equation in the following form:

$$\frac{dH_1}{d\tau_2} = \kappa_1 H_1 + \kappa_2|H_1|^2H_1. \tag{27}$$

Here $\kappa_1 = \kappa_{1,r} + i\kappa_{1,i}$ is the linear complex growth rate and $\kappa_2 = \kappa_{2,r} + i\kappa_{2,i}$ is the complex Landau constant. The real part of this constant determines the type of bifurcation.

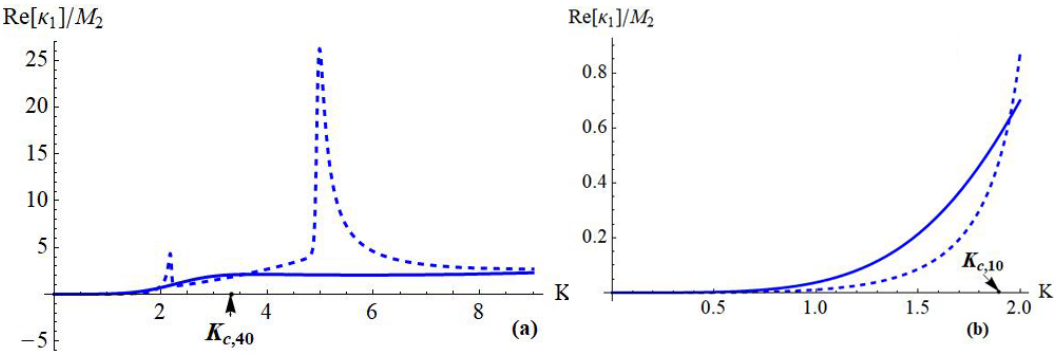

FIG. 6. (a) Real part of the coefficient κ_1 versus wave number K at $\beta = 10$ (solid line) and $\beta = 40$ (blue dashed line). (b) The detailed graphs at $K < 2$. The critical wave numbers for $\beta = 10$ and $\beta = 40$ are marked. Other parameters are $G = 1$, $\tilde{\Sigma} = 1$, $L = 0.003$, and $N = 0.001$.

To obtain the coefficient κ_1 it is sufficient to write the linearized system at third order in the following form:

$$h_{3,\tau_0} - \frac{1}{3}\Delta(Gh_3 - \tilde{\Sigma}\Delta h_3) - \frac{M_0}{2}\Delta(\theta_3 - h_3) - \frac{N}{2}\Delta\gamma_3$$
$$= -\partial_{\tau_2}h_1 + \frac{M_2}{2}K^2(h_1 - \theta_1) + C_1 e^{iKX + i\omega_0\tau_0} + \text{c.c.} + C_2 e^{3i(KX+\omega_0\tau_0)} + \text{c.c.}, \tag{28}$$

$$\theta_{3,\tau_0} - \frac{1}{8}\Delta(Gh_3 - \tilde{\Sigma}\Delta h_3) - \frac{M_0}{6}\Delta(\theta_3 - h_3) - \frac{N}{6}\Delta\gamma_3 - \Delta\theta_3 + \beta(\theta_3 - h_3)$$
$$= -\partial_{\tau_2}\theta_1 + \frac{M_2}{6}K^2(h_1 - \theta_1) + C_5 e^{iKX + i\omega_0\tau_0} + \text{c.c.} + C_6 e^{3i(KX+\omega_0\tau_0)} + \text{c.c.}, \tag{29}$$

$$\gamma_{3,\tau_0} - \frac{1}{2}\Delta(Gh_3 - \tilde{\Sigma}\Delta h_3) - M_0\Delta(\theta_3 - h_3) - (N + L)\Delta\gamma_3$$
$$= -\partial_{\tau_2}\gamma_1 + M_2K^2(h_1 - \theta_1) + C_3 e^{iKX + i\omega_0\tau_0} + \text{c.c.} + C_4 e^{3i(KX+\omega_0\tau_0)} + \text{c.c.} \tag{30}$$

Eliminating the secular terms with $e^{i(KX+\Omega_0\tau_0)}$ and taking into consideration Eqs. (19) and (20), we obtain

$$\frac{\kappa_1}{M_2} = \frac{-K^2(K^2L + i\Omega_0)[(72 + G)K^2 + K^4\tilde{\Sigma} + 48i\Omega_0]}{432\Omega_0^2 - 96i[K^2(3 + G + 3L - M_0 + 3N) + 3\beta + K^4\tilde{\Sigma}]\Omega_0 - \mathcal{D}_3}, \tag{31}$$

where

$$\mathcal{D}_3 = K^2\{[GK^2 + K^4\tilde{\Sigma}][48 + 48L - M_0 + 12N] + 48G\beta + 144[L + N]\beta$$
$$-24K^2[2L(M_0 - 3) + 3M_0 - 6N - 2\beta\tilde{\Sigma}]\}. \tag{32}$$

The expression for κ_2 is given in the Supplemental Material; see Ref. [18].

Formally, Eq. (27) is valid for any K. However, the vicinity of the neutral curve minimum, $K = K_c$, $M = M_0(K_c) = M_c$, is of a special interest. The dependence of the critical values (M_c, K_c) on β is shown in Fig. 4.

Calculation of the real part of coefficient κ_1/M_2 according to Eq. (31) shows that it is positive for all critical wave numbers. That means that the linear instability is developed when $M_2 > 0$, i.e., at the Marangoni number above the linear instability threshold. For example, for $\beta = 10$ the critical wave number and the corresponding Marangoni number are $K_c = 1.90$ and $M_{\text{osc},c} = 10.91$, respectively, and the coefficient $\text{Re}(\kappa_1)/M_2 = 0.57$. In Fig. 6 this case is represented by the solid line. The dashed line in Fig. 6 corresponds to the case of $\beta = 40$, here the critical wave number

and the corresponding Marangoni number are $K_c = 3.31$ and $M_{\mathrm{osc},c} = 25.91$, respectively, and the real part of $\kappa_1/M_2 = 1.83$. For $\beta = 80\,\mathrm{Re}[\kappa_1]/M_2 = 2.59$ the critical wave number and the critical Marangoni number are $K_c = 3.94$ and $M_{\mathrm{osc},c} = 34.98$, respectively.

The coefficient κ_2 was calculated for the same three values of the rescaled Biot number: $\beta = 10$, $\beta = 40$, and $\beta = 80$. At the corresponding values of critical wave numbers $K_c = 1.90$, $K_c = 3.31$, and $K_c = 3.94$, respectively, all the values of κ_2 have negative real part, which means that in all these three cases we have supercritical bifurcations. At $\beta = 10$ we have $\mathrm{Re}(\kappa_2) = -38.6$, at $\beta = 40$ and $\beta = 80$ the value of $\mathrm{Re}(\kappa_2) = -41.7$ and -111, respectively.

Thus, the single traveling wave with $K = K_c$ bifurcates in a supercritical way: the solution $|H_1|^2 = -\kappa_1/\kappa_2 > 0$ exists for $M_2 > 0$. Obviously, it is stable in the framework of Eq. (27).

V. COUNTERPROPAGATING WAVES

A more complex solution of system (2)–(4) is a pair of traveling waves propagating in opposite directions, which has the following form:

$$h_1 = H_{11}(\tau_2)e^{iKX+i\Omega\tau_0} + H_{12}(\tau_2)e^{-iKX+i\Omega\tau_0} + \text{c.c.}, \tag{33}$$

$$\theta_1 = \alpha_1 H_{11}(\tau_2)e^{iKX+i\Omega\tau_0} + \alpha_1 H_{12}(\tau_2)e^{-iKX+i\Omega\tau_0} + \text{c.c.}, \tag{34}$$

$$\gamma_1 = \alpha_2 H_{11}(\tau_2)e^{iKX+i\Omega\tau_0} + \alpha_2 H_{12}(\tau_2)e^{-iKX+i\Omega\tau_0} + \text{c.c.} \tag{35}$$

Here, α_1 and α_2 are defined by Eqs. (19) and (20).

At second order we find the solution in the form

$$h_2 = H_{21}(\tau_2)e^{2iKX+2i\Omega\tau_0} + H_{22}(\tau_2)e^{-2iKX+2i\Omega\tau_0} + I_1(\tau_2)e^{2iKX} + \text{c.c.}, \tag{36}$$

$$\theta_2 = F_{20} + F_{21}(\tau_2)e^{2iKX+2i\Omega\tau_0} + F_{22}(\tau_2)e^{-2iKX+2i\Omega\tau_0} + J_1(\tau_2)e^{2iKX} + J_2(\tau_2)e^{2i\tau_0\Omega_0} + \text{c.c.}, \tag{37}$$

$$\gamma_2 = \Gamma_{21}(\tau_2)e^{2iKX+2i\Omega\tau_0} + \Gamma_{22}(\tau_2)e^{-2iKX+2i\Omega\tau_0} + K_1(\tau_2)e^{2iKX} + \text{c.c.} \tag{38}$$

Here the coefficients can be obtained from the set of the second-order equations. The solvability condition is determined at the third-order system and it is formulated as a set of two Landau equations for amplitudes H_{11} and H_{12}:

$$\frac{dH_{11}}{d\tau_2} = \kappa_1 H_{11} + \kappa_2|H_{11}|^2 H_{11} + \kappa_3|H_{12}|^2 H_{11}, \tag{39}$$

$$\frac{dH_{12}}{d\tau_2} = \kappa_1 H_{12} + \kappa_2|H_{12}|^2 H_{12} + \kappa_3|H_{11}|^2 H_{12}. \tag{40}$$

The system (39), (40) is related to the well-known model of "species competition" (see, e.g., Ref. [19]). Its full analysis is given in Ref. [20], Sec. 5.3, so we present only the results.

This system (39), (40) has three kinds of fixed points: (a) $H_{11} = 0$ and $H_{12} = 0$ is the quiescent state, (b) $H_{11} = 0$, $|H_{12}|^2 = -\mathrm{Re}(\kappa_1)/\mathrm{Re}(\kappa_2)$ and $H_{12} = 0$, $|H_{11}|^2 = -\mathrm{Re}(\kappa_1)/\mathrm{Re}(\kappa_2)$ describe the regime of traveling waves (TWs), and (c) $H_{11} = H_{12} = -\mathrm{Re}(\kappa_1)/\mathrm{Re}(\kappa_2 + \kappa_3)$ is the regime of standing waves (SWs). TWs were studied in Sec. IV, but the analysis here can determine their linear stability with respect to a wider class of disturbances. Because $\mathrm{Re}(\kappa_1) > 0$, the condition for the supercritical bifurcation SW is

$$\mathrm{Re}(\kappa_2 + \kappa_3) < 0.$$

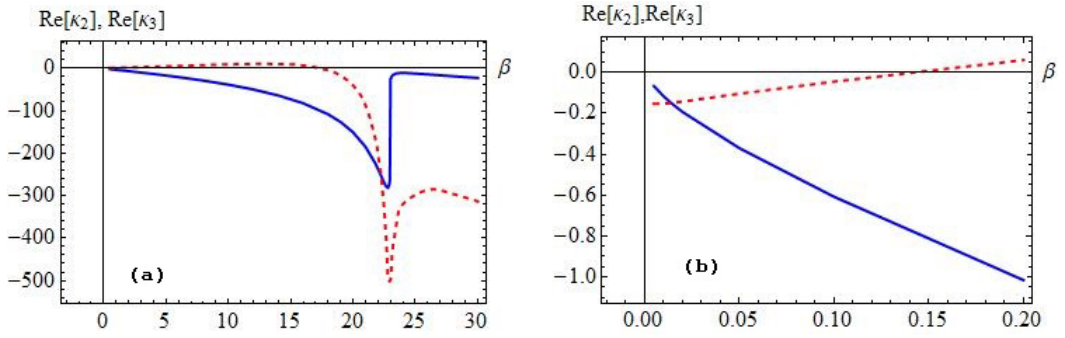

FIG. 7. (a) Real part of the coefficients κ_2 (solid line) and κ_3 (dashed line) versus the Biot parameter at the critical wave numbers. (b) Detailed fragment of panel (a) at small β. Other parameters are $G = 1$, $\tilde{\Sigma} = 1$, $L = 0.003$, and $N = 0.001$.

The difference between the self-interaction coefficient κ_2 and the cross-interaction coefficient κ_3 at the critical points determines the pattern selection. TWs are selected when we have $\mathrm{Re}(\kappa_3) < \mathrm{Re}(\kappa_2)$ and in the opposite case the SWs are stable.

The expression for the cross-interaction coefficient κ_3 is also very cumbersome (see Supplemental Material [18]) and it is presented here only graphically. For comparison we use the same parameters as in the previous section ($G = 1$, $\tilde{\Sigma} = 1$, $L = 0.003$, and $N = 0.001$). First we calculate the coefficients at the same parameters β as in the previous section. We obtain the following data: for $\beta = 10$ the critical wave number is $K_c = 1.9$ and $\mathrm{Re}(\kappa_3) = 8.84$; for $\beta = 40$ the critical wave number is $K_c = 3.31$ and $\mathrm{Re}(\kappa_3) = -428$; and for $\beta = 80$ the critical wave number is $K_c = 3.94$ and $\mathrm{Re}(\kappa_3) = -955$. Just to remind the reader, we have, respectively, $\mathrm{Re}(\kappa_2) = -38.6$ for $\beta = 10$, $\mathrm{Re}(\kappa_2) = -41.7$ for $\beta = 40$, and $\mathrm{Re}(\kappa_2) = -111$ for $\beta = 80$. Thus, in all these cases, SWs bifurcate supercritically. The comparison with the calculated κ_2 obtained earlier for the same critical values shows that in the case with $\beta = 10$ the SW is stable, while for both cases with $\beta = 40$ and $\beta = 80$ the TWs are stable.

To find the value of parameter β where the stability of waves is changed we draw the dependence of the real part of the coefficients κ_2 and κ_3 at the critical wave number on β (see Fig. 7). The solid line represents $\mathrm{Re}(\kappa_2)$ and the dashed line is for the $\mathrm{Re}(\kappa_3)$. The figure shows that, for $\beta < 22.2$, we have $\mathrm{Re}(\kappa_3) > \mathrm{Re}(\kappa_2)$ and standing waves are selected. When $\beta > 22.2$ the stability of the waves is changed and traveling waves are selected.

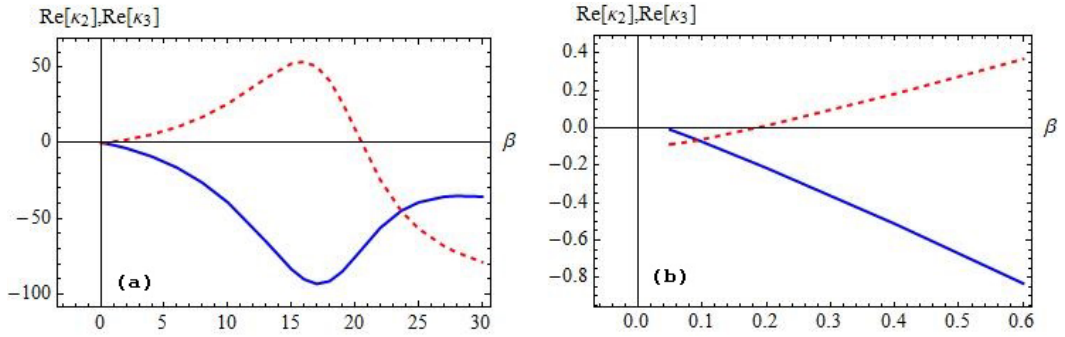

FIG. 8. (a) Real part of the coefficients κ_2 (solid line) and κ_3 (dashed line) versus the Biot parameter at the critical wave numbers. (b) Detailed fragment of panel (a) at small β. Other parameters are $G = 1$, $\tilde{\Sigma} = 1$, $L = 0.003$, and $N = 0.1$.

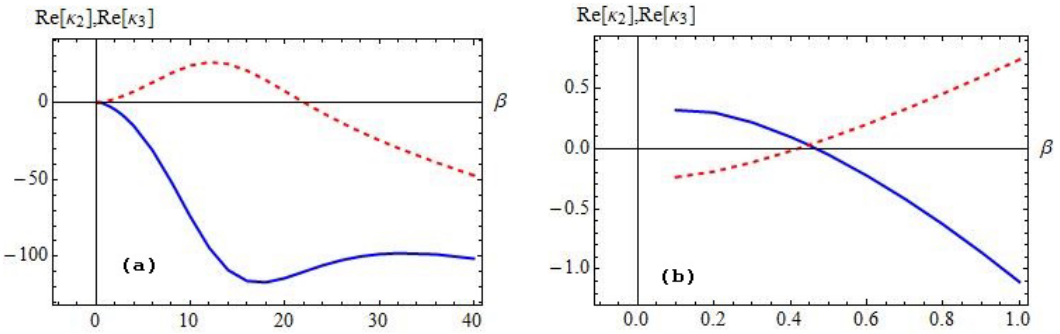

FIG. 9. (a) Real part of the coefficients κ_2 (solid line) and κ_3 (dashed line) versus the Biot parameter at the critical wave numbers. (b) Detailed fragment of panel (a) at small β. Other parameters are $G = 1$, $\tilde{\Sigma} = 1$, $L = 0.003$, and $N = 0.5$.

The calculation shows that, when we diminish the value of parameter β, the selected regimes are changed again. For small β at $N = 0.001$ the SWs are selected only when $\beta > 0.014$, for less small values of β we again have TWs as stable ones [see Fig. 7(b)].

Note that the jump of K_c at $\beta_c = 22.95$ shown in Fig. 4(b) does not lead to a change of the selected wave pattern.

VI. INFLUENCE OF SURFACTANT CONCENTRATION

In this section we consider the influence of the surfactant concentration on the pattern selection of the large-scale Marangoni convection. The elasticity parameter N characterizes this influence. For the linear problem we know that even a small portion of the surfactant changes the marginal curves of the Marangoni large-cell convection. With the growth of the elasticity parameter N, the gap between the monotonic instability boundary and the oscillatory one only increases and the motionless state is stabilized (the marginal stability curves move upward in Fig. 2 when N increases). Here we consider the solution of Eqs. (2)–(4) in the form of traveling or counterpropagating waves for different values of the elasticity parameter.

We work again with the set of Landau equations in the form (39), (40) with greater values of the elasticity number.

Let us take $N = 0.1$. Figure 8 shows how the real part of the self-interaction coefficient, κ_2, (solid line) and the real part of the cross-interaction coefficient, κ_3, (dashed line) vary with the Biot number β.

Again the patterns are selected differently in three different ranges of β. First, for small $\beta < 0.095$ the traveling wave (TW) is selected, in the range $0.095 < \beta < 23.63$ the standing wave (SW) is selected, and for $\beta > 23.63$ the TW is selected again. As in the case $N = 0.001$ considered in the previous section, solutions at $N = 0.1$ bifurcate supercritically. However, the bifurcation type changes at greater values of the elasticity number.

Figure 9 shows the real parts of Landau coefficients κ_2 and κ_3 with parameter β for $N = 0.5$. At $\beta < 0.46$, both kinds of solutions bifurcate subcritically. In the interval $0.46 < \beta < 0.6$ the TW solution bifurcates supercritically ($\mathrm{Re}\kappa_2 < 0$), but the SW solution bifurcates subcritically [$\mathrm{Re}(\kappa_2 + \kappa_3) > 0$]. For $\beta > 0.6$ both kinds of solutions bifurcate supercritically, and the SW pattern is selected.

VII. CONCLUSIONS

Here we have performed the weakly nonlinear analysis for the most dangerous instability mode, the oscillatory one, in the long-wave Marangoni convection which occurs in a nonisothermal liquid

layer covered by an insoluble surfactant. The analysis is carried out for wave number $k \sim \mathrm{Bi}^{1/2}$, where Bi is the Biot number which characterizes the weak heat flux from the free surface.

Two types of solutions were considered. The first type is the traveling wave (TW). The analysis shows that the bifurcation of a TW is typically supercritical near the critical wave number for sufficiently small values of the elasticity parameter. Second, we consider the regime corresponding to a pair of TWs propagating in opposite directions. A set of two Landau equations governing the evolution of the wave amplitudes is derived. The coefficients in the Landau equations are calculated for different Biot numbers. They determine the pattern selection between a possible TW regime and SW regime. With the growth of the elasticity parameter the pattern selection changes from TW to SW and then again to TW. It is found for $N = 0.001$ and $N = 0.1$ that, for considered values of the Biot numbers, SWs bifurcate supercritically. However, at greater values of the elasticity number; for example, at $N = 0.5$, the wave solutions can bifurcate subcritically.

The present work has concentrated on the limit where the solubility of the surfactant has been completely neglected. The analysis of Marangoni convection in the case of soluble surfactant is more complex (see, e.g., Ref. [21]). Note that the oscillatory instability persists.

ACKNOWLEDGMENT

A.A.N. acknowledges support by the Israel Science Foundation (Grant No. 843/18).

[1] A. A. Nepomnyashchy, M. G. Velarde, and P. Colinet, *Interfacial Phenomena and Convection* (Chapman and Hall/CRC Press, London, 2001).

[2] S. Shklyaev and A. Nepomnyashchy, *Longwave Instabilities and Patterns in Fluids* (Birkhäuser, New York, 2017).

[3] A. Oron, S. H. Davis, and S. G. Bankoff, Long-scale evolution of thin liquid films, Rev. Mod. Phys. **69**, 931 (1997).

[4] R. V. Craster and O. K. Matar, Dynamics and stability of thin liquid films, Rev. Mod. Phys. **81**, 1131 (2009).

[5] J. R. Pearson, On convection cells induced by surface-tension gradients, J. Fluid Mech. **4**, 489 (1958).

[6] L. E. Scriven and C. V. Sternling, On cellular convection driven by surface-tension gradients: Effects of mean surface tension and surface viscosity, J. Fluid Mech. **19**, 321 (1964).

[7] J. W. Scanlon and L. A. Segel, Finite-amplitude cellular convection induced by surface tension, J. Fluid Mech. **30**, 149 (1967).

[8] V. V. Pukhnachev, The appearance of thermocapillary effect in a thin liquid layer, in *Hydrodynamics and Heat Mass Transfer of Fluid Flows with a Free Surface* (Institute of Thermophysics SB AS USSR, Novosibirsk, 1985), p. 119 (in Russian).

[9] T. Funada, Nonlinear surface waves driven by the Marangoni instability in a heat transfer system, J. Phys. Soc. Jpn. **56**, 2031 (1987).

[10] S. H. Davis, Rupture of thin liquid films, in *Waves in Fluid Interfaces*, edited by R. E. Meyer (Academic, New York, 1983), p. 291.

[11] A. A. Golovin, A. A. Nepomnyashchy, and L. M. Pismen, Pattern formation in large-scale Marangoni convection with deformable interface, Physica D **81**, 117 (1995).

[12] A. L. Zuev and K. G. Kostarev, Certain peculiarities of the solutocapillary convection, Phys. Usp. **51**, 1027 (2008).

[13] A. Mizev, A. Trofimenko, D. Schwabe, and A. Viviani, Instability of Marangoni flow in the presence of an insoluble surfactant. Experiments, Eur. Phys. J. Spec. Top. **219**, 89 (2013).

[14] A. B. Mikishev and A. A. Nepomnyashchy, Long-wave Marangoni convection in a liquid layer with insoluble surfactant: Linear theory, Microgravity Sci. Technol. **22**, 415 (2010).

[15] A. B. Mikishev and A. A. Nepomnyashchy, Nonlinear large-scale Marangoni convection in a heated liquid layer with insoluble surfactant, Phys. Rev. E **82**, 046306 (2010).
[16] S. Shklyaev, A. A. Alabuzhev, and M. Khenner, Long-wave Marangoni convection in a thin film heated from below, Phys. Rev. E **85**, 016328 (2012).
[17] A. B. Mikishev and A. A. Nepomnyashchy, Amplitude equations for large-scale Marangoni convection in a liquid layer with insoluble surfactant on deformable free surface, Microgravity Sci. Technol. **23**, 59 (2011).
[18] See Supplemental Material at http://link.aps.org/supplemental/10.1103/PhysRevFluids.4.094002 for expressions of coefficients κ_2 and κ_3.
[19] J. D. Murray, *Mathematical Biology* (Springer, New York, 2002).
[20] R. Hoyle, *Pattern Formation. An Introduction to Methods* (Cambridge University Press, Cambridge, 2006).
[21] M. Morozov, A. Oron, and A. Nepomnyashchy, Long-wave Marangoni convection in a layer of surfactant solution: Bifurcation analysis, Phys. Fluids **27**, 082107 (2015).